Direct Observation of Long-Range Assisted Formation of Ag Clusters on Si(111)7 × 7

Ivan Ošťádal,* Pavel Kocán, Pavel Sobotík, and Jan Pudl

Charles University, Faculty of Mathematics and Physics, Department of Electronics and Vacuum Physics, V Holešovičkách 2, 180 00 Praha 8, Czech Republic

(Received 9 June 2005; published 27 September 2005)

Formation of Ag clusters on reconstructed surface Si(111)7 × 7 was for the first time observed in real time during deposition by means of scanning tunneling microscopy. The sequences of images taken at room temperature show mechanisms controlling the growth and behavior of individual Ag adatoms. Obtained data reveal new details of attractive interaction between adsorbates occupying adjacent half-unit cells of the 7 × 7 reconstruction. Time evolution of growth characteristics was simulated by means of a simple model. The growth scenario observed *in vivo* is discussed with respect to previously reported models based on data obtained after finishing the deposition—*post-mortem*.

DOI: 10.1103/PhysRevLett.95.146101 PACS numbers: 68.55.Ac, 68.37.Ef

Processes which control nucleation and thin film growth have been a subject of basic materials science research for decades. Preparation of ordered nanostructures using self-assembling of growing objects [1] is a promising alternative approach in nanotechnology. Growing laterally ordered metal structures on the silicon surfaces is of utmost practical importance due to ubiquitous use of silicon in microelectronic industry. The surface Si(111)7 × 7 consisting of large (2.7 nm) triangular half-unit cells (HUC's) of two different types [faulted (F-HUC's) and unfaulted (U-HUC's)] represents a natural template for growing arrays of identical ordered metal clusters [2,3]. Further development of techniques for manufacturing desirable structures deeply depends on detailed understanding of mechanisms controlling growth for particular combination of materials. Studying growth processes on atomic level is inevitable for such a purpose. The scanning tunneling microscopy (STM) provides unique, real space imaging of the surface with atomic resolution. It has been widely used for studying morphology of surfaces and grown structures for two decades.

Most of STM data on growth were obtained by *in situ* experiments in ultrahigh vacuum (UHV) in the following way: the growth was interrupted, a grown sample quenched and finally transferred to a position suitable for STM measurements [mostly at room temperature (RT)]. The obtained data—images of film structures at various stages of growth—were influenced by structure relaxation during the quenching and a time interval before the STM measurement. Information on growth kinetics can be obtained indirectly; general tendencies are estimated only. Another successful application of STM technique is direct observation of dynamics of thermally activated processes—surface diffusion [4–6] and phase transitions [7,8]. Such experiments require stability of an STM system in desired temperature range and sufficient scanning speed. Temperature is used to control rates of the observed processes. The other challenging step in STM utilization is direct observation of surface during deposition of material. In this case, a scanning STM tip represents a natural obstacle for the flux of the deposited material which results in a screening effect. First experiments on direct STM imaging of film growth (*in vivo*) were focused on epitaxial growth of semiconductor materials at higher temperatures [9,10]. The screening effect of an apex of a scanning STM tip [11] was partially eliminated by enlargement of scanned area (typically hundreds nm). Sufficiently high mobility of adatoms deposited at higher substrate temperature, when a mean free path of diffusing adatoms is comparable with a tip apex radius, further improves compensation of the tip screening. Island growth dynamics, attachment and detachment of adatoms at ''stable'' positions were observed excellently [12]. However, the mobile adatoms cannot be imaged by STM—its movement is too fast with respect to STM scanning speed.

Studies of growth at submonolayer coverage were reported for particular metals [2,3,5,13,14] and even for bimetallic combination [2]. Information on morphology of grown nanostructures and its evolution at various stages of the growth were obtained by *in situ* STM at RT after several hours delay and relaxation of grown structures. Different growth models, based on interpretation of *in situ* STM experiments, describe metal growth kinetics at very low coverages [13–15]. Diffusion parameters of metal adatoms have been obtained independently—from direct observation in STM [4,6].

Here we present STM experiments which—according to our knowledge—for the first time reveal individual behavior of adatoms during deposition of metal on the Si(111)7 × 7 surface, process of nucleation, and island growth at early stages of heteroepitaxial growth at RT. Direct STM observation of growth during metal deposition provided a movie showing dynamics of processes participating at growth.

Experimental.—STM measurements presented here were performed at RT when intercell mobility of diffusing Ag adatoms is sufficiently low [4]. A noncommercial UHV STM system developed by two of authors was used at

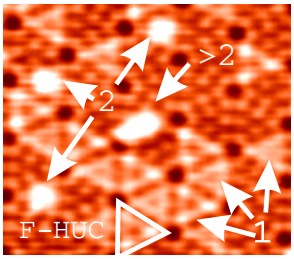

FIG. 1 (color online). Detail of STM image (13×11 nm^2) showing different objects on the surface: monomers (1), dimers (2), and larger clusters (>2). Deposited amount of Ag ~0.6 atoms/HUC.

experiments. The surface was scanned with a rate of 1 image per minute. Si(111) substrates (Sb doped, n-type, resistivity 0.005–0.01 Ω cm) were used. The 7×7 reconstructed surface was obtained using a standard flashing procedure. Ag was deposited on the scanned surface from a miniature tungsten wire evaporator at a distance of 4 cm. A beam of the Ag atoms was defined by means of two apertures (1 mm diameter). Incidental angle of the deposited flux was 30°. The apex shape of a tungsten electrochemically etched tip allowed the deposition of the Ag atoms "under" the STM tip scanning an area of 40×40 nm^2.

The deposition rate was set to a relatively very low value of the order 10^{-5} ML/s (monolayer, 1 ML $= 7.54 \times 10^{14}$ atoms/cm^2). Temperature of the evaporator has been stabilized with negligible delay after switching on the heating current. The thermal drift due to radiation of the evaporator was eliminated by an STM control unit during the whole sequence of STM images covering 2–3 hours of the deposition ~0.1 ML of Ag. We used the tip voltage -2 V; the tunneling current <0.35 nA did not affect intercell hopping of Ag adatoms [see Ref. [4]].

Results.—The following Ag objects can be reliably distinguished on STM images (Fig. 1): monomers (single Ag adatoms) appearing as highlighted triangular HUC's due to fast motion of an Ag adatom inside the HUC [16]; dimers, with a pattern of a bright spot in the position of three Si adatoms central with respect to HUC [16] and clusters composed of more than two Ag atoms (a number of Ag atoms contained in larger clusters cannot be specified accurately on the images at RT [16]). Figure 2 shows evolution of Ag adsorbate on the surface during deposition from monomer population [Fig. 2(a)] to the population of larger clusters [Fig. 2(d)]. Sequences of hundreds of STM images were used for direct identification of atomic processes on the surface. After heating up the evaporator Ag atoms impinge on the sample surface [Fig. 2(a)]. Because of the screening effect of the STM tip the evaporation flux cannot be uniform along the whole scanned area. However, very low gradient of density of occupied HUC's indicates that the very end of the tip has a small diameter of about tens of nanometers (observation of similar tips in a transmission electron microscope showed the tip apex radius of 10–20 nm).

The most important atomic processes observed are hops of Ag adatoms between neighboring HUC's (Fig. 3). The hops to HUC's occupied by single Ag atoms are very rare at RT (<5 events during several hours of observation of an area of ≈ 1000 nm^2) as well as the hops to unoccupied neighboring HUC's. The most frequent process is a hop from the HUC occupied by a single Ag atom to the neighboring HUC with a cluster of at least 2 Ag atoms. It indicates a kind of attractive intercell interaction of the Ag adsorbate. Surprisingly, we found several times a configuration corresponding to hops of a dimer to an adjacent occupied HUC. However, we cannot exclude such process being composed of two separated hops of single Ag atoms.

The attractive intercell interaction can be quantified in a simple way: when the total number of the Ag atoms in positions allowing hops to adjacent HUC's containing at least 2 Ag atoms is n_0, the number n of the atoms hopping within a time interval t is given by an equation $n = n_0[1 - \exp(-t/\tau)]$, where τ is the mean lifetime of an Ag atom in a HUC adjacent to the HUC occupied by an Ag cluster of 2 or more atoms. An analysis of image sequences showed that for $n_0 \approx 50$ suitable positions, 30% or 50% of Ag atoms hop within 3 or 5 min, respectively. It corresponds to a value $\tau = (8 \pm 4)$ min. Effective activation energy E of the process is given by the equation $\tau = \nu_0^{-1} \exp(E/kT)$, where k is the Boltzmann constant, T is the sample temperature, and ν_0 is the frequency prefactor. The value of the activation energy is $E = (0.78 \pm 0.02)$ eV when using the value $\nu_0 = 5 \times 10^{10}$ s^{-1} [an average of experimentally

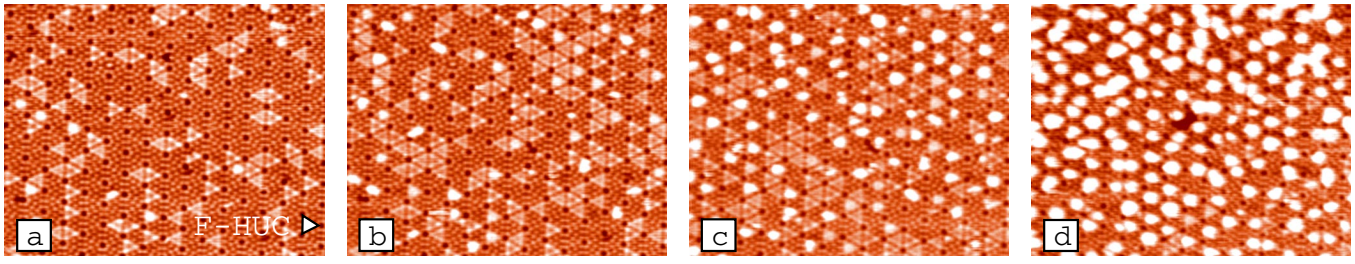

FIG. 2 (color online). Images of the same area taken during deposition after (a) 7 min, (b) 12 min, (c) 24 min, and (d) 92 min from the beginning of growth. Image size 40×30 nm^2. The complete sequence is available on the World Wide Web [20].

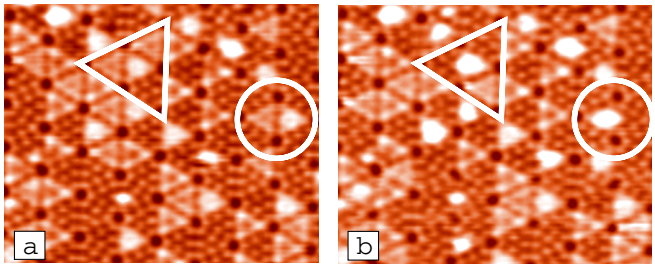

FIG. 3 (color online). Two consecutive images (20×16 nm^2, interval 1 min) showing details of hopping events. Inside the triangle two monomers jump to one of the neighboring larger clusters; inside the circle a dimer moved to a monomer.

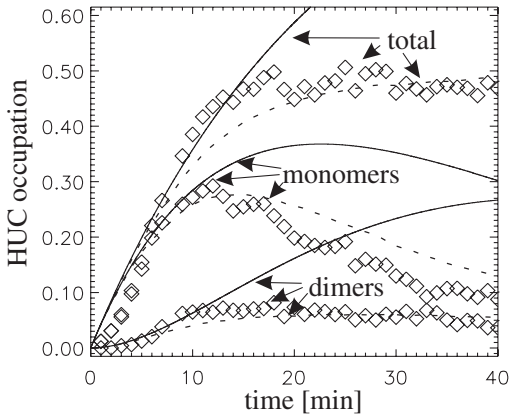

FIG. 4. Time evolution of HUC occupation with respect to monomers and dimers. Diamonds—experimental data, dashed lines—a simple kinetic Monte Carlo model, solid lines—*hit and stick* model, calculated from Eqs. (1)–(3).

obtained values of prefactors for jumps of monomers out of F-HUC's and U-HUC's to an empty HUC [4]].

Two qualitatively different growth regimes can be distinguished on sequences of STM images taken during the deposition at room temperature: (1) *hit and stick* (HS) mode—when a relative number of occupied HUC's is <0.5 no hops of Ag adatoms are observed and the atoms remain at positions of impingement. It is in agreement with long lifetimes τ_F, τ_U of monomers with no clusters in neighboring HUC's: $\tau_F = (6 \pm 2) \times 10^4$ s, $\tau_U = (3.5 \pm 2.0) \times 10^3$ s [reported in Ref. [4]]. The time evolution of HUC occupancies obtained from STM image sequences can be compared with a solution of the set of differential equations:

$$d\theta_1/dt = \gamma R(1 - \theta) - \gamma R\theta_1, \quad (1)$$

$$d\theta_2/dt = \gamma R\theta_1 - \gamma R\theta_2, \quad (2)$$

$$d\theta_{>2}/dt = \gamma R\theta_2, \quad (3)$$

where θ_i represents relative occupancy of HUC's containing i Ag atoms ($\theta_i = n_i/m$, n_i is number of HUC's occupied by i atoms, and m is the number of all HUC's), θ is relative occupancy of HUC's occupied by deposit, $\theta = \theta_1 + \theta_2 + \theta_{>2}$, R is a deposition flux in ML/s, and $\gamma = 23.64$ is a constant equal to number of atoms in ML of Ag per HUC area. The mean value of the flux was estimated from the best fit of the experimental data (Fig. 4) as $(3.0 \pm 0.5) \times 10^{-5}$ ML/s. (2) When clusters containing >2 Ag atoms begin to appear in HUC's adjacent to those with monomers (at relative number of occupied HUC's ≈ 0.5) intercell hops stimulated by Ag clusters start to influence the growth. In this regime the relative coverage increases rather slowly in comparison with the HS regime. Deposited atom impinges with high probability either on an occupied HUC or on adjacent HUC's and hops within several minutes to a HUC occupied by an Ag cluster. In this regime the preference in occupation of F-HUC's (ratio between the occupied F-HUC's and all occupied HUC's) increases up to the final value of ≈ 0.6 which reflects the difference between energy barriers for hops out of F-HUC's and U-HUC's, respectively.

The observed growth has been simulated by a simple kinetic Monte Carlo (KMC) model with HUC's as the smallest units. The only considered processes are deposition (random impingement) and thermally activated hops of monomers to clusters containing ≥ 2 Ag atoms. The hops to clusters of different size were not distinguished. When the fixed value of a frequency prefactor is used, $\nu_0 = 5 \times 10^{10}$ s^{-1}, the model contains only two parameters to be fitted: E_F, E_U—barriers for hops to a cluster from F-HUC and U-HUC, respectively. The corresponding hopping rates can be calculated as $\nu_{F,U} = \nu_0 \exp(-E_{F,U}/kT)$. Results of the KMC simulations are shown in Fig. 4. The best fit of experimental data has been obtained for the barrier energies $E_F = (0.71 \pm 0.02)$ eV and $E_U = (0.76 \pm 0.02)$ eV. The values are in a very good agreement with the effective value of the activation energy estimated from the simple analysis of the monomer mean lifetime τ in HUC's adjacent to a HUC occupied by the Ag cluster. The values are lower than barriers for hops to unoccupied HUC's obtained experimentally in Ref. [4]. The differences, which are 0.10 eV for hops out of F-HUC and 0.17 eV for U-HUC, respectively, quantitatively express influence of clusters in neighboring HUC's on the hopping rate of single Ag adatoms.

The observed behavior of Ag adatoms shows clearly interaction between metal adsorbates resulting in preferential hops of an adatom toward first-neighboring HUC's occupied by metal clusters. The clusters modifying surface mobility have to contain at least 2 Ag adatoms. Surprisingly, the interaction between Ag monomers in adjacent HUC's is negligible at RT. A kind of intercell interaction among metal adsorbates has been indicated by existence of capture zones observed in grown structures on the reconstructed 7×7 surface [Ag [13,17], Pb [5], Y [14], In [2], Tl [3]]. At RT, STM observation of mobile adsor-

bate showed that Pb adatoms hop faster into adjacent occupied HUC's than to empty ones [5]; in the case of Sn only jumps to occupied (monomer) neighboring HUC's were observed [18]. The data reported here agree with models for metal adatom surface mobility with hopping barrier reduced by the attractive nonlocal intercell interaction between adsorbates. The model of *cooperative* diffusion proposed in [14] and discussed in [15] explains well growth characteristics obtained from STM measurements on relaxed structures. The new data obtained here by STM during deposition show that the interaction among adsorbates, at least in case of Ag at RT, is more complex than situation described by the previous models.

The *in vivo* data show that the growth at RT and very low deposited amount (< 0.025 ML, HUC occupancy ≈ 0.5) can be approximated by the *hit and stick* regime. It could not be revealed by standard STM *in situ* measurements and has not been admitted by previous models. A problem of how to explain the preference in occupation of F-HUC's generally found for all studied metals at low coverage was solved in one of models by introducing a mechanism of transient mobility which allows hops of deposited adatoms immediately after arriving on surface [13]. The mechanism of *cooperative* diffusion based on interaction between adsorbates was successfully used in simulation as well [14]. Both models and modifications discussed elsewhere [15] supposed the preference in occupation of F-HUC's arising during the deposition. We have tested that the preference at very low coverage can be entirely explained by deposit relaxation during 2–3 hours before STM observation.

The growth models used previously for simulation of metal heteroepitaxial growth on the Si(111)7 $\times$ 7 surface were focused on intercell mobility of deposited adatoms [coarse grained models [13–15,19]] and were successful in simulation of integral growth characteristics obtained from STM measurements at various substrate temperature, deposition flux, and deposited amount. They provided microscopic parameters of intercell hopping, size of a stable cluster [13], and capacity of HUC's for accommodation of Ag adatoms [19]. The new experimental results presented here show all the models suffered by insufficient description of processes controlling growth at early stages.

Conclusions.—The metal adsorption, diffusion, and cluster nucleation were for the first time directly observed by STM during the deposition at room temperature on the reconstructed Si(111)7 $\times$ 7 surface. The *in vivo* observation revealed the *hit and stick* regime of growth up to a relative coverage ≈ 0.5 followed by formation of clusters via monomer mobility released and controlled by the arising clusters. The measured growth characteristics were interpreted by a simple model covering observed growth regimes. The KMC simulation of cluster formation provided values of hopping barriers between HUC's which reflect barrier height reduction expected due to the nature of an attractive interaction between metal adsorbates. The *in vivo* STM observation of growth during the deposition provides image sequences containing direct information on kinetics of surface processes and time evolution of deposit morphology. It allows us to specify details of growth model with incomparably higher accuracy than by using the standard STM *in situ* observation.

The work is a part of the research plan MSM 0021620834 that is financed by the Ministry of Education of Czech Republic and partly was supported by Projects No. GACR 202/03/0792 and No. GAUK 307/2004/B.

*Electronic address: ivan.ostadal@mff.cuni.cz

[1] C. Teichert, Phys. Rep. **365**, 335 (2002).
[2] J.-L. Li, J.-F. Jia, X.-J. Liang, X. Liu, J.-Z. Wang, Q.-K. Xue, Z.-Q. Li, J. S. Tse, Z. Zhang, and S. B. Zhang, Phys. Rev. Lett. **88**, 066101 (2002).
[3] L. Vitali, M. G. Ramsey, and F. P. Netzer, Phys. Rev. Lett. **83**, 316 (1999).
[4] P. Sobotík, P. Kocán, and I. Ošt'ádal, Surf. Sci. **537**, L442 (2003).
[5] J. M. Gómez-Rodríguez, J. J. Sáenz, A. M. Baró, J. Y. Veuillen, and R. C. Cinti, Phys. Rev. Lett. **76**, 799 (1996).
[6] E. Ganz, S. K. Theiss, I. S. Hwang, and J. Golovchenko, Phys. Rev. Lett. **68**, 1567 (1992).
[7] I. Brihuega, O. Custance, R. Pérez, and J. M. Gómez-Rodríguez, Phys. Rev. Lett. **94**, 046101 (2005).
[8] O. Custance, I. Brihuega, J. Y. Veuillen, J. M. Gómez-Rodríguez, and A. M. Baró, Surf. Sci. **482**, 878 (2001).
[9] T. Hasegawa, M. Kohno, S. Hosaka, and S. Hosoki, Phys. Rev. B **48**, 1943 (1993).
[10] B. Voigtländer and T. Weber, Phys. Rev. Lett. **77**, 3861 (1996).
[11] B. Voigtländer, A. Zinner, and T. Weber, Rev. Sci. Instrum. **67**, 2568 (1996).
[12] B. Voigtländer, M. Kästner, and P. Šmilauer, Phys. Rev. Lett. **81**, 858 (1998).
[13] J. Mysliveček, P. Sobotík, I. Ošt'ádal, T. Jarolímek, and P. Šmilauer, Phys. Rev. B **63**, 045403 (2001).
[14] C. Polop, E. Vasco, J. A. Martín-Gago, and J. L. Sacedón, Phys. Rev. B **66**, 085324 (2002).
[15] E. Vasco, C. Polop, and E. Rodríguez-Cañas, Phys. Rev. B **67**, 235412 (2003).
[16] T. Jarolímek, P. Sobotík, I. Ošt'ádal, and J. Mysliveček, Surf. Sci. **482**, 386 (2001).
[17] P. Sobotík, I. Ošt'ádal, J. Mysliveček, and T. Jarolímek, Surf. Sci. **454-456**, 847 (2000).
[18] O. Custance, I. Brihuega, J. M. Gómez-Rodríguez, and A. M. Baró, Surf. Sci. **482**, 1406 (2001).
[19] P. Kocán, P. Sobotík, I. Ošt'ádal, and M. Kotrla, Phys. Rev. B **69**, 165409 (2004).
[20] http://physics.mff.cuni.cz/kevf/vrstvy/index_eng.htm.